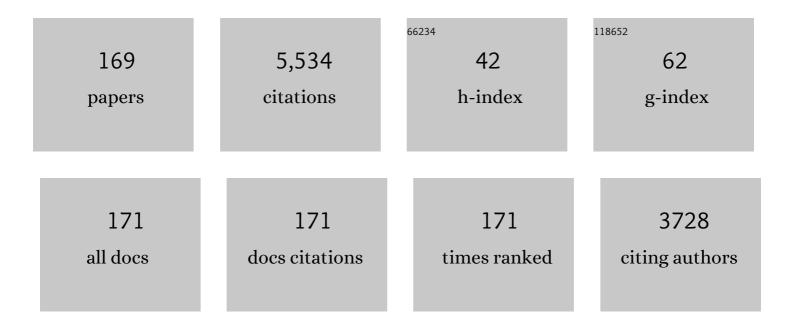
## Li-Min Zheng

List of Publications by Year in descending order

Source: https://exaly.com/author-pdf/9306046/publications.pdf Version: 2024-02-01



LI-MIN THENC

#	Article	IF	CITATIONS
1	Photocontrollable Magnetism and Photoluminescence in a Binuclear Dysprosium Anthracene Complex. Inorganic Chemistry, 2023, 62, 1864-1874.	1.9	11
2	Engineering Heteronuclear Arrays from <scp>Ir<sup>III</sup>â€Metalloligand</scp> and <scp>Co<sup>II</sup></scp> Showing Coexistence of Slow Magnetization Relaxation and Photoluminescence. Chinese Journal of Chemistry, 2022, 40, 931-938.	2.6	4
3	Iridium-lanthanide complexes: Structures, properties and applications. Coordination Chemistry Reviews, 2022, 456, 214367.	9.5	14
4	Dynamic Cantilever Magnetometry of Paramagnetism with Slow Relaxation. Chinese Physics Letters, 2022, 39, 037501.	1.3	0
5	Hydrated metal ions as weak BrÃ,nsted acids show promoting effects on proton conduction. CrystEngComm, 2022, 24, 3886-3893.	1.3	8
6	Mixed-ligated cobalt phosphonates showing slow magnetic relaxation and spin-flop behavior. Journal of Solid State Chemistry, 2022, , 123227.	1.4	0
7	Layered Uranyl Phosphonates Encapsulating Co(II)/Mn(II)/Zn(II) Ions: Exfoliation into Nanosheets and Its Impact on Magnetic and Luminescent Properties. Chemistry - A European Journal, 2022, , .	1.7	2
8	Photoresponsive proton conduction in Zr-based metal–organic frameworks using the photothermal effect. Chemical Communications, 2022, 58, 8372-8375.	2.2	7
9	Thermo- and light-triggered reversible interconversion of dysprosium–anthracene complexes and their responsive optical, magnetic and dielectric properties. Chemical Science, 2021, 12, 929-937.	3.7	43
10	Thermo-induced structural transformation with synergistic optical and magnetic changes in ytterbium and erbium complexes. Chinese Chemical Letters, 2021, 32, 1519-1522.	4.8	11
11	From helices to superhelices: hierarchical assembly of homochiral van der Waals 1D coordination polymers. Chemical Science, 2021, 12, 12619-12630.	3.7	9
12	Cobalt(II)â€dianthracene Frameworks: Assembly, Exfoliation and Properties. Chemistry - an Asian Journal, 2021, 16, 1456-1465.	1.7	8
13	Dysprosium Coordination Polymer Incorporating Dianthracene: Thermoâ€induced Phase Transition Accompanied with Magnetic and Optical Changes. European Journal of Inorganic Chemistry, 2021, 2021, 1565-1570.	1.0	8
14	Anhydrous Superprotonic Conductivity of a Uranyl-Based MOF from Ambient Temperature to 110 °C. , 2021, 3, 744-751.		27
15	Chemically Exfoliated Semiconducting Bimetallic Porphyrinylphosphonate Metal–Organic Layers for Photocatalytic CO <sub>2</sub> Reduction under Visible Light. ACS Applied Energy Materials, 2021, 4, 4319-4326.	2.5	22
16	Homochiral Dysprosium Phosphonate Nanowires: Morphology Control and Magnetic Dynamics. Chemistry - an Asian Journal, 2021, 16, 2648-2658.	1.7	7
17	Heterometallic uranyl-organic frameworks incorporating manganese and copper: Structures, ammonia sorption and magnetic properties. Polyhedron, 2021, 205, 115327.	1.0	7
18	Polar Lanthanide Anthracene Complexes Exhibiting Magnetic, Luminescent and Dielectric Properties. European Journal of Inorganic Chemistry, 2021, 2021, 4207-4215.	1.0	4

#	Article	IF	CITATIONS
19	Dysprosium–dianthracene framework showing thermo-responsive magnetic and luminescence properties. Journal of Materials Chemistry C, 2021, 9, 10749-10758.	2.7	12
20	Layer or Tube? Uncovering Key Factors Determining the Rolling-up of Layered Coordination Polymers. Journal of the American Chemical Society, 2021, 143, 17587-17598.	6.6	10
21	Controllable Macroscopic Chirality of Coordination Polymers through pH and Anionâ€Mediated Weak Interactions. Chemistry - A European Journal, 2021, 27, 16722-16734.	1.7	12
22	Clusterâ€Bridgingâ€Coordinated Bimetallic Metalâ ''Organic Framework as Highâ€Performance Anode Material for Lithiumâ€Ion Storage. Small Structures, 2021, 2, 2100122.	6.9	25
23	Uranyl phosphonates: crystalline materials and nanosheets for temperature sensing. Dalton Transactions, 2021, 50, 17129-17139.	1.6	9
24	Metal-organic nanotubes: Designs, structures and functions. Coordination Chemistry Reviews, 2020, 403, 213083.	9.5	33
25	Luminescent Ir( <scp>iii</scp> )–Ln( <scp>iii</scp> ) coordination polymers showing slow magnetization relaxation. Inorganic Chemistry Frontiers, 2020, 7, 4580-4592.	3.0	23
26	Polar layered coordination polymers incorporating triazacyclononane-triphosphonate metalloligands. Dalton Transactions, 2020, 49, 3758-3765.	1.6	9
27	Metal phosphonates incorporating metalloligands: assembly, structures and properties. Chemical Communications, 2020, 56, 12090-12108.	2.2	36
28	Metal–Metalloligand Coordination Polymer Embedding Triangular Cobalt–Oxo Clusters: Solvent- and Temperature-Induced Crystal to Crystal Transformations and Associated Magnetism. Inorganic Chemistry, 2020, 59, 8935-8945.	1.9	19
29	Chiral metal phosphonates: assembly, structures and functions. Science China Chemistry, 2020, 63, 619-636.	4.2	27
30	Synergetic magnetic and luminescence switching <i>via</i> solid state phase transitions of the dysprosium–dianthracene complex. Journal of Materials Chemistry C, 2020, 8, 7369-7377.	2.7	24
31	Field-induced slow magnetic relaxation in low-spin <i>S</i> = 1/2 mononuclear osmium( <scp>v</scp> ) complexes. Dalton Transactions, 2020, 49, 4084-4092.	1.6	16
32	Cyclic Lanthanide-based Molecular Clusters: Assembly and Single Molecule Magnet Behavior. Acta Chimica Sinica, 2020, 78, 34.	0.5	19
33	Interplay of anthracene luminescence and dysprosium magnetism by steric control of photodimerization. Dalton Transactions, 2019, 48, 13769-13779.	1.6	24
34	Incorporating Paramagnetic Ir <sup>IV</sup> Cl <sub>6</sub> <sup>2–</sup> in H-Bonded Networks of Metal-Phosphonate Hydrate: Slow Magnetic Relaxation and Proton Conduction. Crystal Growth and Design, 2019, 19, 4836-4843.	1.4	10
35	Cyclometalated Iridium(III) Complexes Incorporating Aromatic Phosphonate Ligands: Syntheses, Structures, and Tunable Optical Properties. ACS Omega, 2019, 4, 16543-16550.	1.6	11
36	Two- and Three-Dimensional Heterometallic Ln[Ru2-α-Ammonium Diphosphonate] Nets: Structures, Porosity, Magnetism, and Proton Conductivity. Inorganic Chemistry, 2019, 58, 14034-14045.	1.9	15

#	Article	IF	CITATIONS
37	Hofmann Metal–Organic Framework Monolayer Nanosheets as an Axial Coordination Platform for Biosensing. ACS Applied Materials & Interfaces, 2019, 11, 12986-12992.	4.0	32
38	Polymorphic layered copper phosphonates: exfoliation and proton conductivity studies. Dalton Transactions, 2019, 48, 6539-6545.	1.6	15
39	Syntheses, crystal structures and magnetic properties of a series of luminescent lanthanide complexes containing neutral tetradentate phenanthroline-amide ligands. Inorganic Chemistry Frontiers, 2019, 6, 1442-1452.	3.0	20
40	Octahedral erbium and ytterbium ion encapsulated in phosphorescent iridium complexes showing field-induced magnetization relaxation. Journal of Magnetism and Magnetic Materials, 2019, 484, 139-145.	1.0	8
41	Homochiral iron(ii)-based metal–organic nanotubes: metamagnetism and selective nitric oxide adsorption in a confined channel. Chemical Communications, 2019, 55, 2825-2828.	2.2	25
42	From a layered iridium( <scp>iii</scp> )–cobalt( <scp>ii</scp> ) organophosphonate to an efficient oxygen-evolution-reaction electrocatalyst. Chemical Communications, 2019, 55, 13920-13923.	2.2	15
43	Changes in magnetic order through two consecutive dehydration steps of metal-phosphonate diamond chains. RSC Advances, 2019, 9, 31911-31917.	1.7	2
44	Proton conductive metal phosphonate frameworks. Coordination Chemistry Reviews, 2019, 378, 577-594.	9.5	300
45	Lanthanide anthracene complexes: slow magnetic relaxation and luminescence in Dy <sup>III</sup> , Er <sup>III</sup> and Yb <sup>III</sup> based materials. Dalton Transactions, 2019, 48, 2735-2740.	1.6	32
46	Coupling photo-, mechano- and thermochromism and single-ion-magnetism of two mononuclear dysprosium–anthracene–phosphonate complexes. Chemical Communications, 2018, 54, 3278-3281.	2.2	39
47	Iridium(III)-Based Metal–Organic Frameworks as Multiresponsive Luminescent Sensors for Fe <sup>3+</sup> , Cr <sub>2</sub> O <sub>7</sub> 2–, and ATP <sup>2–</sup> in Aqueous Media. Inorganic Chemistry, 2018, 57, 1079-1089.	1.9	104
48	Bioinspired Engineering of Cobalt-Phosphonate Nanosheets for Robust Hydrogen Evolution Reaction. ACS Catalysis, 2018, 8, 3895-3902.	5.5	69
49	Na <sub>2</sub> Ir <sup>IV</sup> Cl <sub>6</sub> : Spin–Orbital-Induced Semiconductor Showing Hydration-Dependent Structural and Magnetic Variations. Inorganic Chemistry, 2018, 57, 13252-13258.	1.9	15
50	Counteranion Modulated Crystal Growth and Function of One-Dimensional Homochiral Coordination Polymers: Morphology, Structures, and Magnetic Properties. Inorganic Chemistry, 2018, 57, 12143-12154.	1.9	17
51	Temperature controlled formation of polar copper phosphonates showing large dielectric anisotropy and a dehydration-induced switch from ferromagnetic to antiferromagnetic interactions. Chemical Communications, 2018, 54, 6276-6279.	2.2	5
52	Reversible SCâ€SC Transformation involving [4+4] Cycloaddition of Anthracene: A Singleâ€Ion to Singleâ€Molecule Magnet and Yellowâ€Green to Blueâ€White Emission. Angewandte Chemie, 2018, 130, 8713-8717.	1.6	13
53	Reversible ON–OFF switching of single-molecule-magnetism associated with single-crystal-to-single-crystal structural transformation of a decanuclear dysprosium phosphonate. Chemical Science, 2018, 9, 6424-6433.	3.7	54
54	Dynamic Motion of Organic Ligands in Polar Layered Cobalt Phosphonates. Chemistry - A European Journal, 2018, 24, 13495-13503.	1.7	5

#	Article	IF	CITATIONS
55	Reversible SCâ€SC Transformation involving [4+4] Cycloaddition of Anthracene: A Singleâ€Ion to Singleâ€Molecule Magnet and Yellowâ€Green to Blueâ€White Emission. Angewandte Chemie - International Edition, 2018, 57, 8577-8581.	7.2	97
56	Homochiral Erbium Coordination Polymers: Salt-Assisted Conversion from Triple to Quadruple Helices. Crystal Growth and Design, 2018, 18, 4045-4053.	1.4	13
57	Defective Metal–Organic Frameworks Incorporating Iridiumâ€Based Metalloligands: Sorption and Dye Degradation Properties. Chemistry - A European Journal, 2017, 23, 6615-6624.	1.7	44
58	Chiral expression from molecular to macroscopic level via pH modulation in terbium coordination polymers. Nature Communications, 2017, 8, 2131.	5.8	35
59	Formation Mechanism and Reversible Expansion and Shrinkage of Magnesiumâ€Based Homochiral Metal–Organic Nanotubes. Chemistry - A European Journal, 2017, 23, 1086-1092.	1.7	17
60	Proton Conductivities Manipulated by the Counter-Anions in 2D Co-Ca Coordination Frameworks. European Journal of Inorganic Chemistry, 2016, 2016, 4476-4482.	1.0	13
61	Cyclic Singleâ€Molecule Magnets: From Evenâ€Numbered Hexanuclear to Oddâ€Numbered Heptanuclear Dysprosium Clusters. European Journal of Inorganic Chemistry, 2016, 2016, 3184-3190.	1.0	12
62	Selfâ€assembly of a Linear Ni <sub>9</sub> Tripleâ€helical Supramolecule with Dominant Ferromagnetic Interactions. Chemistry - an Asian Journal, 2016, 11, 2021-2024.	1.7	7
63	Successive Phase Transition, Dielectric Ordering, and Liquid Crystalline Behavior of Simple (Laurylammonium)(Phenyl Phosphates) Salts. Journal of Physical Chemistry B, 2016, 120, 6761-6770.	1.2	9
64	Polymorphic Lanthanide Phosphonates Showing Distinct Magnetic Behavior. Inorganic Chemistry, 2016, 55, 5297-5304.	1.9	19
65	Magnetic materials based on 3d metal phosphonates. Coordination Chemistry Reviews, 2016, 319, 63-85.	9.5	109
66	Enantiopure phosphonic acids as chiral inducers: homochiral crystallization of cobalt coordination polymers showing field-induced slow magnetization relaxation. Chemical Communications, 2016, 52, 6877-6880.	2.2	21
67	Facile synthesis of a water stable 3D Eu-MOF showing high proton conductivity and its application as a sensitive luminescent sensor for Cu <sup>2+</sup> ions. Journal of Materials Chemistry A, 2016, 4, 16484-16489.	5.2	99
68	Enantioenriched Cobalt Phosphonate Containing Δ-Type Chains and Showing Slow Magnetization Relaxation. Inorganic Chemistry, 2016, 55, 9521-9523.	1.9	11
69	Homochiral mononuclear Dy-Schiff base complexes showing field-induced double magnetic relaxation processes. Dalton Transactions, 2016, 45, 690-695.	1.6	18
70	Cyclic single-molecule magnets: from the odd-numbered heptanuclear to a dimer of heptanuclear dysprosium clusters. Chemical Communications, 2016, 52, 2314-2317.	2.2	41
71	Multiple-Step Humidity-Induced Single-Crystal to Single-Crystal Transformations of a Cobalt Phosphonate: Structural and Proton Conductivity Studies. Inorganic Chemistry, 2016, 55, 3706-3712.	1.9	49
72	Lanthanide salen-type complexes exhibiting single ion magnet and photoluminescent properties. Dalton Transactions, 2016, 45, 2974-2982.	1.6	47

#	Article	IF	CITATIONS
73	Chirality―and pHâ€Controlled Supramolecular Isomerism in Cobalt Phosphonates and Its Impact on the Magnetic Behavior. Chemistry - A European Journal, 2015, 21, 17336-17343.	1.7	17
74	Co–Ca Phosphonate Showing Humidity-Sensitive Single Crystal to Single Crystal Structural Transformation and Tunable Proton Conduction Properties. Chemistry of Materials, 2015, 27, 8116-8125.	3.2	137
75	pH-controlled polymorphism in a layered dysprosium phosphonate and its impact on the magnetization relaxation. Chemical Communications, 2015, 51, 2649-2652.	2.2	28
76	Enlarging the ring by incorporating a phosphonate coligand: from the cyclic hexanuclear to octanuclear dysprosium clusters. Dalton Transactions, 2015, 44, 14208-14212.	1.6	15
77	Modulating the microporosity of cobalt phosphonates via positional isomerism of co-linkers. CrystEngComm, 2015, 17, 8926-8932.	1.3	11
78	A cryogenic luminescent ratiometric thermometer based on a lanthanide phosphonate dimer. Journal of Materials Chemistry C, 2015, 3, 8480-8484.	2.7	87
79	Lanthanide phosphonates with pseudo-D <sub>5h</sub> local symmetry exhibiting magnetic and luminescence bifunctional properties. Inorganic Chemistry Frontiers, 2015, 2, 558-566.	3.0	56
80	Cobalt and copper pyridylmethylphosphonates with two- and three-dimensional structures and field-induced magnetic transitions. Dalton Transactions, 2015, 44, 19256-19263.	1.6	4
81	Homochiral metal phosphonate nanotubes. Chemical Communications, 2015, 51, 15141-15144.	2.2	26
82	Lanthanide-based Single Molecule Magnets. Acta Chimica Sinica, 2015, 73, 1091.	0.5	40
83	Switching on Single-Molecule-Magnet Behavior in MnIII-Schiff Base Out-of-Plane Dimers by the Phosphonate Terminal Ligand. European Journal of Inorganic Chemistry, 2014, 2014, 1042-1050.	1.0	9
84	Homochiral Cobalt Phosphonates Containing Δâ€Type Chains with a Tunable Interlayer Distance and a Fieldâ€Induced Phase Transition. Chemistry - A European Journal, 2014, 20, 17137-17142.	1.7	26
85	Polar metal phosphonate containing unusual μ4-OH bridged double chains showing canted antiferromagnetism with large coercivity. Chemical Communications, 2014, 50, 3979.	2.2	37
86	Exfoliated layered copper phosphonate showing enhanced adsorption capability towards Pb ions. Chemical Communications, 2014, 50, 10622.	2.2	20
87	A layered erbium phosphonate in pseudo-D5h symmetry exhibiting field-tunable magnetic relaxation and optical correlation. Chemical Communications, 2014, 50, 7621.	2.2	83
88	A luminescent heptanuclear DyIr6 complex showing field-induced slow magnetization relaxation. Chemical Communications, 2014, 50, 8356.	2.2	36
89	Control of the Singleâ€Molecule Magnet Behavior of Lanthanideâ€Diarylethene Photochromic Assemblies by Irradiation with Light. Chemistry - A European Journal, 2014, 20, 12502-12513.	1.7	78
90	Heterometallic 3d–4f Coordination Polymers Based on 1,4,7-Triazacyclononane-1,4,7-triyl-tris(methylenephosphonate). Inorganic Chemistry, 2014, 53, 6042-6047.	1.9	21

#	Article	IF	CITATIONS
91	M2(pbtcH)(phen)2(H2O)2 [M(II)=Co, Ni]: Mixed-ligated metal phosphonates based on 5-phosphonatophenyl-1,2,4-tricarboxylic acid showing double chain structures. Chinese Chemical Letters, 2014, 25, 835-838.	4.8	16
92	Enhancing Proton Conduction in 2D Co–La Coordination Frameworks by Solid-State Phase Transition. Journal of the American Chemical Society, 2014, 136, 9292-9295.	6.6	144
93	Synthesis and evaluation of c(RGDyK)-coupled superparamagnetic iron oxide nanoparticles for specific delivery of large amount of doxorubicin to tumor cell. Journal of Nanoparticle Research, 2013, 15, 1.	0.8	2
94	Dy(III) Single-Ion Magnet Showing Extreme Sensitivity to (De)hydration. Inorganic Chemistry, 2013, 52, 8342-8348.	1.9	60
95	Solvent Responsive Magnetic Dynamics of a Dinuclear Dysprosium Singleâ€Molecule Magnet. Chemistry - A European Journal, 2013, 19, 9619-9628.	1.7	60
96	Reaction of an anthracene-based cyclic phosphonate ester with trimethylsilyl bromide unexpectedly generating two phosphonates: syntheses, crystal structures and fluorescent properties. RSC Advances, 2013, 3, 4001.	1.7	5
97	Racemic metal phosphonates based on 1-phosphonomethyl-2-benzimidazol-piperidine. CrystEngComm, 2013, 15, 10316.	1.3	10
98	Diruthenium( <scp>iii</scp> , <scp>iii</scp> ) diphosphonate with a spin ground state S = 2. Dalton Transactions, 2013, 42, 3429-3433.	1.6	22
99	Breathing Effect in a Cobalt Phosphonate upon Dehydration/Rehydration: A Singleâ€Crystalâ€toâ€Singleâ€Crystal Study. Chemistry - A European Journal, 2013, 19, 16394-16402.	1.7	40
100	Cobalt and copper phosphinates based on N-(phosphinomethyl)iminodiacetic acid: supramolecular layered structures and magnetic properties. CrystEngComm, 2012, 14, 4699.	1.3	7
101	Supramolecular Isomerism of Oneâ€Dimensional Copper(II) Phosphonate and Its Influence on the Magnetic Properties. ChemPlusChem, 2012, 77, 1087-1095.	1.3	31
102	Isostructural lanthanide oxalatophosphonates Ln(5pm8hqH3)(C2O4)1.5(H2O)·2H2O [Ln(iii) = Eu, Gd, Tb, Dy] (5pm8hqH3 = 5-phosphonomethyl-8-hydroxyquinoline): structures, magnetic and fluorescent properties. RSC Advances, 2012, 2, 6680.	1.7	15
103	An enantioenriched vanadium phosphonate generated via asymmetric chiral amplification of crystallization from achiral sources showing a single-crystal-to-single-crystal dehydration process. Chemical Communications, 2012, 48, 6565.	2.2	39
104	A Racemic Polar Cobalt Phosphonate with Weak Ferromagnetism. Chemistry - A European Journal, 2012, 18, 10839-10842.	1.7	32
105	Enhanced Magnetic Hardness in a Nanoscale Metal–Organic Hybrid Ferrimagnet. Chemistry - A European Journal, 2012, 18, 9534-9542.	1.7	33
106	Co3(2-OOCC6H4PO3)2(H2O)3·H2O: A layered metal phosphonate showing reversible dehydration–rehydration behavior and ferrimagnetism. Dalton Transactions, 2011, 40, 1307.	1.6	29
107	Cobalt and Manganese Diphosphonates with One-, Two-, and Three-Dimensional Structures and Field-Induced Magnetic Transitions. Inorganic Chemistry, 2011, 50, 2278-2287.	1.9	48
108	Tuning the Spin State of Cobalt in a Co–La Heterometallic Complex through Controllable Coordination Sphere of La. Angewandte Chemie - International Edition, 2011, 50, 5504-5508.	7.2	45

#	Article	IF	CITATIONS
109	Magnetization Relaxation in a Threeâ€Dimensional Ligated Cobalt Phosphonate Containing Ferrimagnetic Chains. Chemistry - A European Journal, 2011, 17, 3579-3583.	1.7	44
110	The solid state reactions of o-aminobenzoic acid with Zn(II), Cu(II), Ni(II), Mn(II) acetate hydrate at room temperature. Chinese Journal of Chemistry, 2010, 12, 243-247.	2.6	1
111	Pillared Layered Metal Phosphonates Showing Fieldâ€Induced Magnetic Transitions. European Journal of Inorganic Chemistry, 2010, 2010, 895-901.	1.0	8
112	Lanthanide oxalatophosphonates with two- and three-dimensional structures. Journal of Solid State Chemistry, 2010, 183, 1159-1164.	1.4	14
113	Metal diphosphonates with double-layer and pillared layered structures based on N-cyclohexylaminomethanediphosphonate. Journal of Solid State Chemistry, 2010, 183, 1588-1594.	1.4	14
114	A pH responsive electrochemical switch sensor based on Fe(notpH3) [notpH6=1,4,7-triazacyclononane-1,4,7-triyl-tris(methylene-phosphonic acid)]. Talanta, 2010, 83, 145-148.	2.9	8
115	Zn3(4-OOCC6H4PO3)2: A polar metal phosphonate with pillared layered structure showing SHG-activity and large dielectric anisotropy. Dalton Transactions, 2010, 39, 8606.	1.6	25
116	Homochiral Lanthanide Phosphonates with Brick-Wall-Shaped Layer Structures Showing Chiroptical and Catalytical Properties. Inorganic Chemistry, 2009, 48, 1901-1905.	1.9	57
117	Functional Interface of Ferric Ion Immobilized on Phosphonic Acid Terminated Self-Assembled Monolayers on a Au Electrode for Detection of Hydrogen Peroxide. Journal of Physical Chemistry C, 2009, 113, 3746-3750.	1.5	28
118	Mixed-valent manganese phosphonate clusters prepared under microwave-assisted and ambient conditions. Dalton Transactions, 2009, , 5029.	1.6	18
119	Lanthanide Carboxyphosphonates Ln(O3PCH2â^'NC5H9â^'COO)(H2O)2·xH2O with Open Framework Structures Containing Parallelogram-like Channels. Crystal Growth and Design, 2009, 9, 4445-4449.	1.4	16
120	Ag(i)-mediated formation of pyrophosphonate coupled with C–C bond cleavage of acetonitrile. Chemical Communications, 2009, , 2893.	2.2	40
121	Tuning the field-induced magnetic transition in a layered cobalt phosphonate by reversible dehydration-hydration process. Chemical Communications, 2009, , 3023.	2.2	40
122	Layered copper compounds based on 4-(3-bromothienyl)phosphonate (BTP): weak ferromagnetism observed in [Cu2(4,4′-bpy)0.5(BTP)2]·H2O. Dalton Transactions, 2009, , 8548.	1.6	28
123	Homochiral zinc phosphonates with layered and open framework structures using polycarboxylate as second linkers. Dalton Transactions, 2009, , 9837.	1.6	31
124	Metal phosphonates based on (4-carboxypiperidyl)-N-methylenephosphonate: in situ ligand cleavage and metamagnetism in Co3(O3PCH2-NHC5H9-COO)2(O3PCH2-NC5H10)(H2O). Dalton Transactions, 2009, , 2746.	1.6	22
125	LiF-assisted crystallization of zinc 4-carboxyphenylphosphonates with pillared layered structures. CrystEngComm, 2009, 11, 1674.	1.3	23
126	[M(OOCC6H4PO3H)(H2O)] (M(II) = Mn, Co, Ni): layered metal phosphonates showing variable magnetic behavior. CrystEngComm, 2009, 11, 1255.	1.3	30

#	Article	IF	CITATIONS
127	Syntheses, structures and catalytic properties of one-dimensional lanthanide-dotp compounds [dotpH8=1,4,7,10-tetraazacyclododecane-1,4,7,10-tetrakis-(methylenephosphonic acid)]. Inorganic Chemistry Communication, 2008, 11, 1075-1078.	1.8	17
128	Copper diphosphonates with zero-, one- and two-dimensional structures: ferrimagnetism in layer compound Cu3(ImhedpH)2·2H2O [ImhedpH4 = (1-C3H3N2)CH2C(OH)(PO3H2)2]. Dalton Transactions, 2008, , 5008.	1.6	40
129	Structure and magnetism of a linear trimanganese (III, II, III) complex based on benzoate and Schiff-base ligands. Journal of Coordination Chemistry, 2008, 61, 2814-2822.	0.8	8
130	Polymorphism in Homochiral Zinc Phosphonates. Inorganic Chemistry, 2008, 47, 5525-5527.	1.9	47
131	Zinc 4-Carboxyphenylphosphonates with Pillared Layered Framework Structures Containing Large 12-Membered Rings Built Up from Tetranuclear Zn <sub>4</sub> Clusters and CPO <sub>3</sub> Linkages. Crystal Growth and Design, 2008, 8, 2950-2953.	1.4	41
132	Chiral-Layered Metal Phosphonate Formed via Spontaneous Resolution Showing Dehydration-Induced Antiferromagnetic to Ferromagnetic Transformation. Inorganic Chemistry, 2008, 47, 10211-10213.	1.9	34
133	Cobalt diphosphonate with a new double chain structure exhibiting field-induced magnetic transition. Dalton Transactions, 2007, , 4681.	1.6	32
134	Microwave-assisted hydrothermal syntheses of metal phosphonates with layered and framework structures. Dalton Transactions, 2007, , 4222.	1.6	16
135	Tridecanuclear and Docosanuclear Manganese Phosphonate Clusters with Slow Magnetic Relaxation. Inorganic Chemistry, 2007, 46, 5459-5461.	1.9	59
136	Lanthanide Diruthenium(II,III) Compounds Showing Layered and PtS-Type Open Framework Structures. Inorganic Chemistry, 2007, 46, 8524-8532.	1.9	68
137	Anion-Directed Self-Assembly of Lanthanide–notp Compounds and Their Fluorescence, Magnetic, and Catalytic Properties. Chemistry - A European Journal, 2007, 13, 2333-2343.	1.7	96
138	Three-Dimensional Lanthanide(III)–Copper(II) Compounds Based on an Unsymmetrical 2-Pyridylphosphonate Ligand: An Experimental and Theoretical Study. Chemistry - A European Journal, 2007, 13, 4759-4769.	1.7	75
139	Copper and cadmium phosphonates based on 2-quinolinephosphonate. Solid State Sciences, 2007, 9, 686-692.	1.5	9
140	Incorporation of Triazacyclononane into the Metal Phosphonate Backbones. Inorganic Chemistry, 2006, 45, 1124-1129.	1.9	57
141	Dodecanuclear Manganese(III) Phosphonates with Cage Structures. Inorganic Chemistry, 2006, 45, 59-65.	1.9	75
142	Template- and pH-Directed Assembly of Diruthenium Diphosphonates with Different Topologies and Oxidation States. Inorganic Chemistry, 2006, 45, 4205-4213.	1.9	44
143	Na3Ru2(hedp)2â‹4H2O: A mixed valent diruthenium diphosphonate with three-dimensional structure. Solid State Sciences, 2006, 8, 1041-1045.	1.5	4
144	Metal Phosphonates Based on {[(Benzimidazol-2-ylmethyl)imino]bis(methylene)}bis(phosphonic Acid): Syntheses, Structures and Magnetic Properties of the Chain Compounds [M{(C7H5N2)CH2N(CH2PO3H)2}](M = Mn, Fe, Co, Cu, Cd). European Journal of Inorganic Chemistry, 2006, 2006, 1830-1837.	1.0	36

#	Article	IF	CITATIONS
145	Synthesis and characterization of two metal phosphonates with 3D structures: Cui2Cull[(3-C5H4N)CH(OH)PO3]2 and Zn[(3-C5H4N)CH(OH)PO3]. New Journal of Chemistry, 2005, 29, 721.	1.4	23
146	Syntheses, Structures, and Magnetic Properties of Mixed-Valent Diruthenium(II,III) Diphosphonates with Discrete and One-Dimensional Structures. Inorganic Chemistry, 2005, 44, 4309-4314.	1.9	54
147	Mixed-Valent Diruthenium Diphosphonate with Kagomé Structure. Inorganic Chemistry, 2005, 44, 6921-6923.	1.9	49
148	One-Dimensional Cobalt Diphosphonates Exhibiting Weak Ferromagnetism and Field-Induced Magnetic Transitions. Inorganic Chemistry, 2004, 43, 2151-2156.	1.9	76
149	Syntheses and Structures of Layered Copper(II) Diphosphonates with Mixed Ligands. European Journal of Inorganic Chemistry, 2003, 2003, 726-730.	1.0	22
150	Novel Layered Ruthenium Diphosphonate Containing a Mixed Valent Diruthenium Paddlewheel Core. Inorganic Chemistry, 2003, 42, 2827-2829.	1.9	36
151	[Cu(tn)]3[W(CN)8]2·3H2O and [Cu(pn)]3[W(CN)8]2·3H2O: Two Novel Cu(II)â^W(V) Cyano-Bridged Two-Dimensional Coordination Polymers with Metamagnetism. Chemistry of Materials, 2003, 15, 2094-2098.	3.2	55
152	Synthesis, crystal structure and magnetic properties of a Cull–WV/IVbimetallic complex with a novel open framework structure. Dalton Transactions, 2003, , 3283-3287.	1.6	31
153	{M(C5H4N)CH(OH)PO3}(H2O)Â(M = Mn, Fe, Co): layered compounds based on [hydroxy(4-pyridyl)methyl]phosphonate. Dalton Transactions, 2003, , 953-956.	1.6	14
154	Metamagnetic Copper(II) Diphosphonates with Layered Structures. Chemistry of Materials, 2002, 14, 3143-3147.	3.2	62
155	Syntheses, crystal structures and magnetic properties of manganese(ii)-hedp compounds involving alkylenediamine templates (hedp = 1-hydroxyethylidene-diphosphonate). Dalton Transactions RSC, 2002, , 2752-2759.	2.3	46
156	Novel Coordination Polymer Containing a Mixed Valence Copper(I,II) Phosphonate Unit: CuI2CuII(hedpH2)2(4,4â€~-bpy)2·2H2O (hedp = 1-Hydroxyethylidenediphosphonate). Inorganic Chemistry, 2002, 41, 4084-4086.	1.9	68
157	A cyano-bridged MnIIMoV bimetallic ferrimagnet with a novel moniliform structure. Dalton Transactions RSC, 2002, , 2805.	2.3	44
158	A novel Cu(II)-W(V) bimetallic assembly magnet {[Cu(en)2]3[W(CN)8]2·H2O}â <sup>*</sup> ž (en = ethylenediamir cube-like W8Cu12 units from a coordinated anion template self-assembly reactionElectronic supplementary information (ESI) available: selected hydrogen bonding parameters in 1 (Table S1) and perspective view showing the three linkages for the title compound (Fig. S1). See http://www.rsc.org/suppdata/nj/b1/b108791f/. New Journal of Chemistry, 2002, 26, 485-489.	ie) with 1.4	47
159	Crystal structures and magnetic properties of two octacyanometalate-based tungstate(v)–copper(ii) bimetallic assemblies. New Journal of Chemistry, 2002, 26, 1190-1195.	1.4	28
160	TOWARDS THE CONSTRUCTION OF OPEN FRAMEWORK STRUCTURES OF COPPER PHOSPHONATES AND THE MAGNETIC STUDIES. , 2002, , .		0
161	Cu4{CH3C(OH)(PO3 )2}2(C4H4N2)(H2O)4: a novel, three-dimensional copper diphosphonate with metamagnetismElectronic supplementary information (ESI) available: views of structure 1, temperature dependence of ac magnetic susceptibility and field dependence of magnetization of 1. See http://www.rsc.org/suppdata/cc/b1/b106780i/. Chemical Communications. 2001 2346-2347.	2.2	87
	Syntheses, structures and magnetic properties of two copper(li) diphosphonates:		10 76 50

162 [NH3(CH2)2NH3]2[Cu2(hedp)2]·H2O and [NH3CH(CH3)CH2NH3]2[Cu2(hedp)2] (hedp =) Tj ETQq0 0 0 rgBT / @ arlock 1@ 1 f 50 57 T

#	Article	IF	CITATIONS
163	Zinc Diphosphonates Templated by Organic Amines:Â Syntheses and Characterizations of [NH3(CH2)2NH3]Zn(hedpH2)2·2H2O and [NH3(CH2)nNH3]Zn2(hedpH)2·2H2O (n= 4, 5, 6) (hedp =) Tj ETQ0	1 <b>1.90.7</b>	843 <b>1⁄4</b> rgBT / <mark>O</mark> \

Syntheses and Structures of Transition Metal-hedp Compounds and the Template Influences (hedp =) Tj ETQq0 0 0.39 BT /Overlock 10 Tf

165	Title is missing!. Transition Metal Chemistry, 1999, 24, 346-349.	0.7	4
166	Template-Directed One- and Two-Dimensional Copper(II) Diphosphonates:Â Structures and Characterizations of (NH4)2Cu3(hedp)2(H2O)4, [NH3(CH2)4NH3]Cu3(hedp)2·2H2O, and [NH2(C2H4)2NH2]Cu3(hedp)2(hedp = 1-Hydroxyethylidenediphosphonate). Inorganic Chemistry, 1999, 38, 5061-5066.	1.9	39
167	[NH3(CH2)4NH3]Fe2[CH3C(OH)(PO3)(PO3H)]2·2H2O: A Novel Iron(II) Diphosphonate with a Supramolecular Open Network Structure. Inorganic Chemistry, 1999, 38, 4618-4619.	1.9	56
168	Solid State Reactions of Dimethylglyoxime with Nickel Acetate at Close to Room Temperature. Synthesis and Reactivity in Inorganic, Metal Organic, and Nano Metal Chemistry, 1995, 25, 1091-1099.	1.8	0
169	Studies on the solid state reactions of coordination conpounds. XLVIII. The effect of KSCN on the thermal decomposition of cobalt(III)â€ammine complexes. Chinese Journal of Chemistry, 1993, 11, 225-230.	2.6	О